Dynamic Impact Effects on Spent Fuel Assemblies*

M.C. Witte, R.C. Chun, M.W. Schwartz

Lawrence Livermore National Laboratory, Livermore, California, United States of America

INTRODUCTION

Spent fuel can be stored at a reactor site in accordance with 10 CFR 72. One method of storage is to use a cask to contain and shield the spent fuel in a dry, inert environment. These large casks are subjected to many operations n the storage process which include loading of the spent fuel in a storage pool, lifting the cask out of the pool, and transporting the cask to a storage area. During these operations, the cask could be dropped and impact a hard surface or object. In addition, the cask could tip over onto the storage pad because of natural phenomena such as a tornado, earthquake or flood. The impact of the cask could damage the spent fuel that is contained inside of the cask. Storage casks are designed and licensed to withstand accident impact loads and to contain within regulatory limits all radioactive material even when it is assumed that the claddings of the spent fuel rods fail during the impact. While there is no regulatory requirement to maintain fuel integrity under accident conditions, it is of interest to assess the ability of the fuel rod cladding to resist such loads.

Objective

The objective of this study is to assess the effects of dynamic impacts to be expected from cask drop or tipover incidents on the integrity of fuel rod cladding for zircalloy-clad light-water-reactor spent fuel assemblies during cask handling and storage. This paper presents the results of an earlier study conducted for the United States Nuclear Regulatory Commission [Chun, et al., 1987].

Approach

A variety of light-water-reactor fuel assembly designs are in use in the United States. The major types are manufactured by Westinghouse, Combustion Engineering, Babcock & Wilcox, and General Electric. The relevant design parameters for each of these fuel assemblies are shown in Table 1 [Greene 1980].

All the different types of rods may be idealized as beams or columns depending upon the loading configuration. In the case of an end drop, the inertial forces load the rod as a column having intermediate supports at each spacer grid. The limit load is that at which the

* This work was supported by the U.S. Nuclear Regulatory Commission under a Memorandum of Understanding with the U.S. Department of Energy.

fuel rod segment between the supports becomes unstable. The segment selected for analysis is the lowest one since it must support the entire weight of the cladding. It is assumed that the fuel pellets do not transfer their weight to cladding. The length to radius-of-gyration ratio of the column is such that Euler buckling applies. The axial critical buckling load is computed from

$$P_{cr} = \frac{C\pi^2 EI}{\ell^2},$$

where ℓ = length of the fuel rod segment between the spacer grids
E = modulus of elasticity of the zircalloy cladding
I = moment of inertia of the cladding neglecting the fuel pellets
C = a constant reflecting the end conditions of the column. A pinned, pinned condition is assumed.

The pressure of the fill gas within the fuel rod causes an additional load. Since this pressure produces tensile stresses in the cladding, it reduces the compressive stresses caused by the end drop impact. However, since small pin holes in the cladding might occur during operation and allow the gas to escape, the tensile stresses are neglected in determining the magnitude of the critical buckling load.

For the side drop, the fuel rods are idealized as continuous beams supported at each spacer grid. Continuous beam theory is used to determine the maximum bending moments and corresponding stresses in the cladding. In this case, fuel gas internal pressure must be assumed to be present and the resulting axial tensile stress added to the bending tensile stress. The gas pressure is conservatively assumed to be 2250 psi. The limit state is the yield strength of the zircalloy. The maximum g load caused by the side impact is the load that corresponds to the yield stress.

MATERIAL PROPERTIES

This section establishes the basis for assuming particular material properties. The value of some of the parameters used in the analysis are temperature dependent. Since the critical buckling load is proportional to the modulus of elasticity that decreases with temperature, conservatism dictates that the maximum temperature over the design life of the storage cask should be used. The maximum temperature during dry storage is not expected to exceed 380°C [Chin and Madsen, 1983]. Consequently, allowable g loads will be based upon this temperature, with the expectation that the ability of the zircalloy to absorb impact loads without rupture will increase as the temperature decreases with time.

The weight density (ρ_w) of both Zircalloy-2 and Zircalloy-4 is very close to the weight density of Zirconium itself. Ross [1980] lists the density as, $\rho_w = 0.234$ lb/in^3.

The Young's modulus for a typical Zircalloy-4 PWR cladding is illustrated as a function of temperature by Hagrman [1979]. Thus, at 380°C (653°K), $E_{Zr\text{-}4} = 7/.2 \times 10^{10}$ Pa = 10.4×10^6 psi. We assume that Zircalloy-2 has the same Young's modulus as Zircalloy-4.

The yield strength of zircalloy is substantially increased at the high strain rates resulting from cask drop on rigid targets. The strain rate during a cask drop is expected to be at least 0.5 in/in/sec.

Experimental tests on irradiated Zircalloy-4 cladding specimens provided by General Electric [1982] indicate that at 750°F (399°C), a fast neutron fluence of 2.5×10^{21} nvt and a strain rate of 0.00042 in/in/sec, the yield strength is 50,500 psi. This reference also indicates that the yield strength will increase by 10,000 psi per order of faster strain rate. Consequently, the yield stress determined by low rate testing should be increased by 30,000 psi to 80,500 psi.

Again, it is assumed that Zircalloy-2 has the same yield strength as Zircalloy-4.

ANALYSIS

The method of analysis is illustrated here with two examples. The Westinghouse 15 x 15 (7 spacer grids) is used here for illustration.

End Drop

The axial critical buckling load of a column was given previously. Using the parameters listed in Tables 1 and 2, and using C = 1 for the pinned-pinned condition, with

$W = 1.2434$ lb
$E = 10.4 \times 10^6$ psi
$I = 7.14 \times 10^{-4}$ in^4
$\ell = 24$"
then $P_{CR} = 127$ lb.

Assuming conservatively, the whole claddings weight is on top of the last section between spacer grids, the g-load necessary for axial Euler buckling is:

$$g_{\text{axial buckling}} = \frac{127}{1.2434} = 102$$

Side Drop

The lateral loading is

$$W = \frac{1420b}{204 \times 144 \text{ in.}} = .04834 \text{ lb/in per rod.}$$

From Marks' Handbook [1978], the maximum moment in a continuous, uniformly loaded beam over equal spans is $.106\, w\ell^2$. Then, for the Westinghouse 15 x 15 case,

$$M = (.106)(.04834)(24)^2 = 2.95 \text{ in-lb}$$

$$\sigma_{\text{bending}} = \frac{Mr}{I} = \frac{(2.95)(0.211)}{7.14 \times 10^{-4} \text{ in}^4} = 871 \text{ psi.}$$

Assuming the maximum pressure inside the fuel is 2,250 psi, there is a constant tension of

$$\sigma_{\text{axial}} = \frac{pr}{2t} = 7350 \text{ psi.}$$

Hence, the necessary g-load for the fuel to reach the yield strength is

$$g_{\text{yield for sidedrop}} = \frac{\sigma_y - \sigma_{\text{axial}}}{\sigma_{\text{bending}}} = \frac{80{,}500 - 7{,}350}{871} = 84.$$

Based on the Handbook of Structural Stability [1971], yielding occurs in this case well before the tube will flatten by instability.

RESULTS AND DISCUSSION

Of all the fuel assemblies analyzed, the weakest appears to be the 17 x 17 Westinghouse fuel assembly primarily because it has the worst combination of the longest unsupported length and the thinnest cladding wall thickness. Nevertheless, it can sustain a static load in bending equivalent to 63 g's at 380°C without exceeding the yield strength of the cladding at that temperature. Realistically, the temperature of the fuel rods will decrease rather rapidly depending upon the duration of in-pool storage prior to storage cask loading. Consequently, the strength of the cladding will increase as the temperature decreases which will be reflected in higher allowable g loadings. After about one year in dry storage, older fuel will consistently remain at a higher temperature. Conservatism dictates that the allowable impact load levels be based upon the older fuel. Table 2 shows the variation of Young's modulus and yield strength with time in dry storage. The effect upon allowable g loads is shown in Figs. 1 and 2 which describe, respectively, the allowable g's for end drop and side drop.

A summary of all the calculated results is shown in Table 3.

The conservative approach to establishing allowable g loads on the spent fuel rods implies a significant, though difficult to quantify at this time, margin between yielding of the cladding and gross rupture. On the positive side is the observation that the total elongation value for zircalloy does not change with strain rate so that its ductility appears to be independent of the level of g loading. On the other hand, the increase in yield strength with strain rate appears to be confirmed only for a 600°-675°F temperature range. Since the increase in yield strength with strain rate may not be as great at lower temperatures, no credit was taken for this effect upon room temperature and full credit for strain rate at the maximum storage temperature.

It is important to emphasize that the g loadings shown in Figs. 1 and 2 are static loadings. These should be compared with the loads indicated by an analysis of the entire fuel rod, basket, and target dynamic system.

CONCLUSION

The analysis of the capability of spent fuel rods to resist impact loads caused by storage cask accidents indicates that, for the most vulnerable fuel assembly, axial buckling varies from 82 g's at initial storage to 95 g's after twenty years' storage. In a side drop, no yielding is expected below 63 g's at initial storage to 74 g's after twenty years' storage. For storage casks designed to limit loads at or below these g levels, it is not likely that damage will occur to the spent fuel rods. In any event, even if the rods were damaged at higher loadings, the storage casks are designed to prevent radioactive releases from exceeding regulatory limits under accident conditions.

REFERENCES

Baumeister, T., et al., Marks' Standard Handbook for Mechanical Engineers, eighth edition (1978).

Chin, B.A., and Madsen, N.H., *Deformation and Fracture Maps for Predicting the Failure Behavior of Spend Fuel Cladding*. In Proceedings of Spend Fuel/Cladding Reaction during Dry Storage, NUREG/CR-0049, sponsored by U.S. Nuclear Regulatory Commission, Gaithersburg, MD (1983).

Chun, R.C., Witte, M.C., and Schwartz, M.W., *Dynamic Impact Effects on Fuel Assemblies*, Lawrence Livermore National Laboratory, UCID-21246 (1987).

Hagrman, D.L., et al., *Matpro-Version II - A Handbook of Material Properties for Use in the Analysis of Light Water Reactor Fuel Rod Behavior*, NUREG/CR-0497 (1979).

Ross, R.B., *Metallic Materials Specification Handbook*, Spon, London (1980).

Column Research Committee of Japan, *Handbook of Structural Stability*, Corona Publishing Company (1971).

Consolidated Safety Analysis Report for IF300 Shipping Cask, General Electric Company, NEDO-10084-2F (1982).

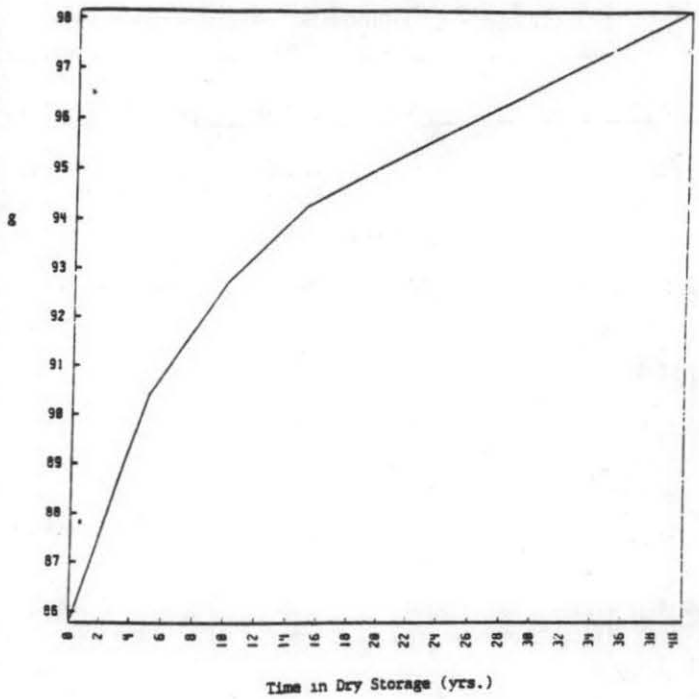

Figure 1. G-values for axial buckling of a Westinghouse 17 x 17 arrayed fuel assembly assuming 5-year-old-fuel.

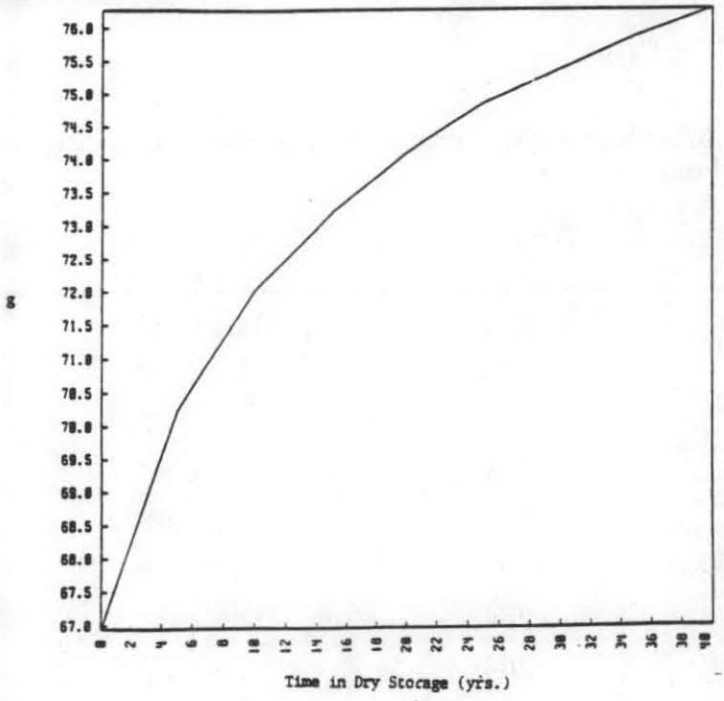

Figure 2. G-values for side-drop yielding of a Westinghouse 17 x 17 arrayed fuel assembly assuming 5-year-old fuel.

Table 1 Mechanical design parameters.

	Westinghouse		Combustion Engineering		Babcock & Wilcox		General Electric	
Rod Array	15x15	17x17	14x14	16x16	15x15	17x17	7x7	8x8
Assembly Weight (lb.)	1420	1450	1280	1446	1516	1484	600	600
Fuel Rods Number per Assembly	204	264	176	236	208	264	40	55
Fueled Length (in.)	144.0	144.0	136.7	150.0	144.0	143.0	144.0	144.0
OD (in.)	0.422	0.374	0.440	0.382	0.430	0.379	0.570	0.493
Clad Thickness (in.)	0.030	0.0225	0.026	0.025	0.0265	0.0235	0.035	0.035
Clad Material	Zr-4	Zr-4	Zr-4	Zr-4	Zr-4	Zr-4	Zr-2	Zr-2
Number of Spacers	7	7	9	12	8	8	7	7

Table 2 Young's Modulus and yield strength versus time in dry storage of a 5-year-in-pool fuel rod.

Time in Dry Storage (years)	Temperature °F	Young's Modulus (psi)	Yield Stress (psi)
0	615.	11.1×10^6	84,371.
5	486.	11.7×10^6	88,071.
10	415.	12.0×10^6	90,107.
15	369.	12.2×10^6	91,426.
20	334.	12.3×10^6	92,429.
25	304.	12.4×10^6	93,290.
30	284.	12.5×10^6	93,863.
35	264.	12.6×10^6	94,437.
40	248.	12.7×10^6	94,896.

Table 3 Calculations of G-loads for axial buckling and for yielding at side drop.

	Westinghouse		Combustion Engineering		Babcock & Wilcox		General Electric	
Rod Array	15x15	17x17	14x14	16x16	15x15	17x17	7x7	8x8
$\ell = \frac{\text{Fueled length}}{\text{No. of Spacers -1}}$	24.	24.	17.09	13.64	20.57	20.43	24.	24.
E (psi)	10.4×10^6	10.4×10^6	10.4×10^6	10.4×10^6	10.4×10^6	10.4×10^6	10.4×10^6	10.4×10^6
σ_y (psi)	80,500	80,500	80,500	80,500	80,500	80,500	80,500	80,500
r_o (in.)	0.211	0.187	0.220	0.191	0.215	0.1895	0.285	0.2465
r_i (in.)	0.181	0.1645	0.194	0.166	0.1885	0.166	0.250	0.2115
$A = \pi(r_o^2 - r_i^2)(in^2)$	0.0369	0.248	0.0338	0.0280	0.0336	0.0262	0.0588	0.0504
$I = \frac{1}{4}\pi(r_o^4 - r_i^4)(in^4)$	7.14×10^{-4}	3.85×10^{-4}	7.27×10^{-4}	4.49×10^{-4}	6.87×10^{-4}	4.16×10^{-4}	2.11×10^{-3}	1.33×10^{-3}
W = 0.234 x A x Fueled length (lb.)	1.2434	0.8357	1.0812	0.9828	1.1322	0.8767	1.9813	1.6983

Table 3 Calculations of G-loads for axial buckling and for yielding at side drop (cont).

	Westinghouse		Combustion Engineering		Babcock & Wilcox		General Electric	
$w = \frac{\text{Assembly wt.}}{(\#\text{ Rods})\ (\text{Fueled Length})}$ (lb./in.)	0.04834	0.03814	0.05320	0.04085	0.05061	0.03931	0.10417	0.07576
$r = \frac{1}{2}(r_o + r_i)$ (in.)	0.196	0.1758	0.207	0.1785	0.2018	0.1778	0.2675	0.229
$\sigma_{axial} = \frac{2{,}250r}{2t}$ (psi)	7,350.	8,790.	8,957.	8,033.	8,567.	8,512.	8,598.	7,361
$M_{max} = 0.106w\ell^2$ (lb.-in.)	2.9459	2.3243	1.6439	0.8041	2.2656	1.7359	6.3482	4.6169
$\sigma_{bending} = \frac{M_{max}\, r_o}{I}$ (psi)	870.57	1,128.95	497.47	342.06	709.03	790.75	857.46	855.69
$P_{cr} = \frac{\pi^2 EI}{\ell^2}$ (lb.)	127.24	68.61	255.50	247.72	166.66	102.31	341.82	215.46
$g_{\text{axial buckling}} = \frac{P_{cr}}{W}$	102	82	236	252	147	116	172	126
$g_{\text{yield for sidedrop}} = \frac{\sigma_y - \sigma_{axial}}{\sigma_{bending}}$	84	63	143	211	101	91	83	85